ARTICLE

OBC
www.rsc.org/obc

Nucleophilic displacement on 4-nitrophenyl dimethyl phosphinate by ethoxide ion: alkali metal ion catalysis and mechanism

Erwin Buncel,*[a] Kendall G. Albright[a] and Ikenna Onyido[b]

[a] *Department of Chemistry, Queen's University, Kingston, Canada K7L 3N6*

[b] *Department of Chemistry and Center for Agrochemical Technology, University of Agriculture, Makurdi, Nigeria*

Received 19th November 2003, Accepted 8th January 2004
First published as an Advance Article on the web 28th January 2004

We report on a spectrophotometric kinetic study of the effect of Li^+ and K^+ cations on the ethanolysis of 4-nitrophenyl dimethylphosphinate (**4a**) in ethanol at 25 °C. The nucleophilic displacement reaction of **4a** with LiOEt and KOEt in the absence and presence of 18-crown-6 ether (18-C-6) furnished observed first-order rate constants which increase in the order EtO^- < KOEt < LiOEt. The kinetic data are analyzed in terms of a scheme which assigns concurrent kinetic activity to free ethoxide and metal alkoxide, to obtain the second-order rate coefficients for reaction of the metal ion–ethoxide pairs, k_{MOEt}. Derived δG_{ip}, δG_{ts} and ΔG_{cat} values quantify ground state and transition state stabilization by the metal ions to give $\delta G_{ts} > \delta G_{ip}$ for Li^+ and $\delta G_{ts} \sim \delta G_{ip}$ for K^+. These results indicate moderate catalysis by Li^+, with **4a** manifesting lesser susceptibility to catalysis than other substrates previously studied. Second-order rate constants for the reaction of the aryl dimethylphosphinates **4a**–**f** with free EtO^- were obtained from plots of log k_{obs} *vs.* [KOEt], measured in the presence of excess 18-C-6. Hammett plots with σ and σ° substituent constants give significantly better correlation of rates than σ^- and yield a moderately large $\rho(\rho^\circ)$ value; this is interpreted in terms of a stepwise mechanism involving rate-limiting formation of a pentacoordinate intermediate. Comparison of the present results with those of Williams on the aqueous alkaline hydrolysis of $Me_2P(O)$–OPhX and $Ph_2P(O)$–OPhX esters, establishes the rationale for a change in mechanism in the more basic EtO^-/EtOH nucleophile/solvent system by a stepwise mechanism instead of a concerted one in aqueous base. Structure–reactivity correlations following Jencks show that the change in mechanism is accounted for by cross interactions between the nucleophile and the leaving group in the transition state. The observed duality of mechanism is rationalized on the basis of the More O'Ferrall–Jencks diagram, as a spectrum of transition states covering a wide range of nucleophile and leaving group basicities.

Introduction

Transfer of the phosphoryl group is an important biological reaction which is directly involved in energy transport and transmission of genetic information in living systems.[1,2] Studies of uncatalyzed and enzymatic phosphoryl transfer have been undertaken in various laboratories in an effort to understand the mechanism of the biological process.[3] Many enzymes involved in the process are known to require metal ion co-factors.[4] As a consequence, several *kinetically labile* and *substitution inert* metal complexes have been investigated as models of the metalloenzymes that mediate in phosphate ester hydrolysis.[4,5] Attention has also been directed at the effects of added metal salts on these reactions.[6] These investigations, however, have involved mainly divalent cations such as Mg^{2+}, Ca^{2+}, Zn^{2+}, Mn^{2+}, Co^{2+}, Cu^{2+}, Fe^{2+}, Pt^{2+}, *etc.*, and have focused largely on the reactions of phosphate esters. Recently, however, reports have appeared of a very large catalytic effect by La^{3+} on the methanolysis of phosphate di- and triesters.[7]

Kinetic investigations of the effects of alkali metal ions have been few. Alkali metal ions are ubiquitous in biological systems and are implicated in a number of vital physiological roles; for instance, the Na^+/K^+ pump is intimately linked to ATP hydrolysis.[8] It was therefore important that in-depth studies of alkali metal ion effects in phosphoryl transfer and related reactions be undertaken to aid an understanding of the role of these metal ions in chemical and biological systems. Such studies were initiated in our laboratories, as part of the investigations of the influence of alkali metal ions on nucleophilic displacement reactions at carbon, phosphorus and sulfur centers.[9–13]

We have reported[9] an unexpected catalysis of the ethanolysis of 4-nitrophenyl diphenylphosphinate, **1**, by alkali metal ions, with the selectivity order of catalytic activity $Li^+ > Na^+ > K^+$. A similar selectivity order was observed[10a] in the catalysis of the ethanolysis of 4-nitrophenyl diphenyl phosphate, **2**, although the magnitude of catalysis was less than that recorded for **1**. In the ethanolysis of the phosphonate ester, 4-nitrophenyl phenylphosphonate, **3**, the kinetic data are consistent with multiple alkali metal ion catalysis.[10b] In order to understand the trend of reactivity in these systems and to characterize the nature of the transition state in these reactions, it became necessary to explore the structural diversity of substrates and their response to catalysis by alkali metal ions. The present paper is concerned with the investigation of the catalytic effects of alkali metal ions on the reaction of ethoxide ion with 4-nitrophenyl dimethylphosphinate, **4a**, for comparison with the results already obtained with **1**–**3**. The reactions of the esters **4a**–**f** were also studied in the presence of the complexing agent 18-crown-6 ether, with a view to probing the electronic effects of substituents on the uncatalyzed reaction, and to aid in the description of the structure of the transition state in these processes.

The results presented herein show moderate and weak catalysis by Li^+ and K^+, respectively, of the nucleophilic displacement on **4a** by ethoxide. The relative stabilization of the initial and transition states by the metal ions has been quantified. It is shown that Li^+ stabilizes the transition state better than the initial state.

The result of the Hammett correlation supports a stepwise mechanism involving a pentacoordinate intermediate for the ethanolysis of these phosphinates. Structure–reactivity considerations reveal variations in transition state (TS) structure with changes in nucleophile and leaving group basicities. These variations in TS structure account for a spectrum of transition states and the observed duality of mechanisms in the nucleophilic displacement reactions of phosphinate esters.

DOI: 10.1039/b314886f

Table 1 Kinetic data for the reaction of **4a** with LiOEt and KOEt in anhydrous ethanol at 25.0 °C

MOEt	10^2 [MOEt]$_0$/M	10^2 [EtO$^-$]$_{eq}$/M	k_{obs}/s^{-1}	k_{obs}/[EtO$^-$]$_{eq}$ (M^{-1} s^{-1})
LiOEt	0.525	0.315	2.00	634
	1.046	0.505	4.43	877
	2.092	0.785	9.42	1200
	3.138	1.004	16.02	1596
	4.184	1.189	21.29	1791
	5.230	1.353	27.84	2059
KOEt	0.485	0.365	1.32	363
	1.031	0.650	2.88	443
	2.002	1.036	5.59	538
	3.034	1.362	7.97	586
	3.882	1.594	9.77	615
	5.036	1.874	12.76	682

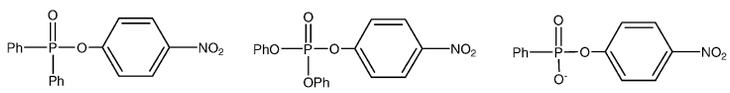

1 **2** **3**

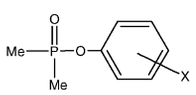

4

(a): X = 4-NO_2
(b): X = 3-NO_2
(c): X = 4-$COCH_3$
(d): X = 4-Cl
(e): X = H
(f): X = 4-CH_3

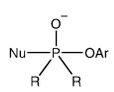

5

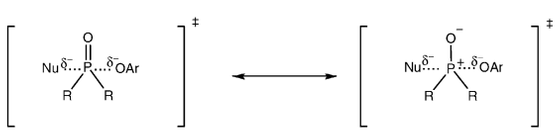

6 **6a**

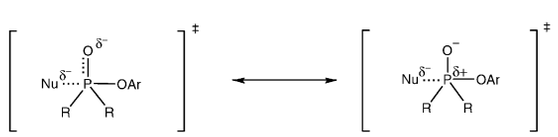

7 **7a**

Results

The rates of ethanolysis of **4a** with LiOEt and KOEt in anhydrous ethanol were determined spectrophotometrically at 25 °C under pseudo-first-order conditions. First-order rate constants, k_{obs}, were reckoned from linear plots of log $(A_\infty - A_t)$ *vs.* time. The results are given in Table 1. The reaction of the substrate with KOEt in the presence of a two-fold excess of 18-C-6 was also investigated (see Table 2). Data in Tables 1 and 2 are shown graphically in Fig. 1 in which the qualitative order of reactivity EtO$^-$ < KOEt < LiOEt is evident.

In order to obtain a Hammett correlation of rates, the kinetics of the reactions of KOEt with the aryl dimethylphosphinate esters **4b**–**f** were also investigated in the presence of excess 18-C-6, at a constant ratio of [18-C-6]/[KOEt] = 2. The results of these experiments are presented in Table 3. In a complementary experiment, the effect of added 18-C-6 was examined for the reaction of **4e** with KOEt, to further ascertain that reaction in the presence of the complexing agent involves free ions. The data are given in Table 4 and plotted in Fig. 2. The rate decreased linearly as a function of [18-C-6] at constant [KOEt], until the addition of one equivalent of the complexing agent relative to KOEt. Further additions of the complexing agent beyond this point had no effect on k_{obs}.

Discussion

Kinetic form and evidence for catalysis by alkali metal ions

The plots shown in Fig. 1 demonstrate linearity for the reaction of **4a** with KOEt in the presence and absence of 18-C-6, while the reaction with LiOEt exhibits upward curvature. The slope of the k_{obs} *vs.* [KOEt] plot for the reaction of **4a** is slightly smaller in the presence of 18-C-6 than in the absence of the complexing agent (Fig. 1), revealing a marginal difference in reactivity between the two species, KOEt ion pair and free EtO$^-$.

In solvents of moderate polarity such as ethanol, free (solvated) ions are in equilibrium with ion paired species due to competition between electrostatic and ion–solvent interactions.[14] Certain S_N2 displacement processes at saturated carbon centers in such solvents exhibit characteristic downward curvatures in plots of *k vs.* [Nu],[15] contrary to what is observed for the reaction of **4a** with LiOEt. The downward curvature has been interpreted as the participation of the ion-paired species

Table 2 Kinetic data for the reaction of **4a** with KOEt in anhydrous ethanol at 25.0 °C in the presence of 2-fold excess 18-C-6

10^2 [KOEt]/M	10^2 [18-C-6]/M	k_{obs}/s^{-1}
1.031	2.359	2.52
2.002	4.132	4.95
3.034	5.966	7.34
3.640	7.967	8.95
4.854	9.830	11.25

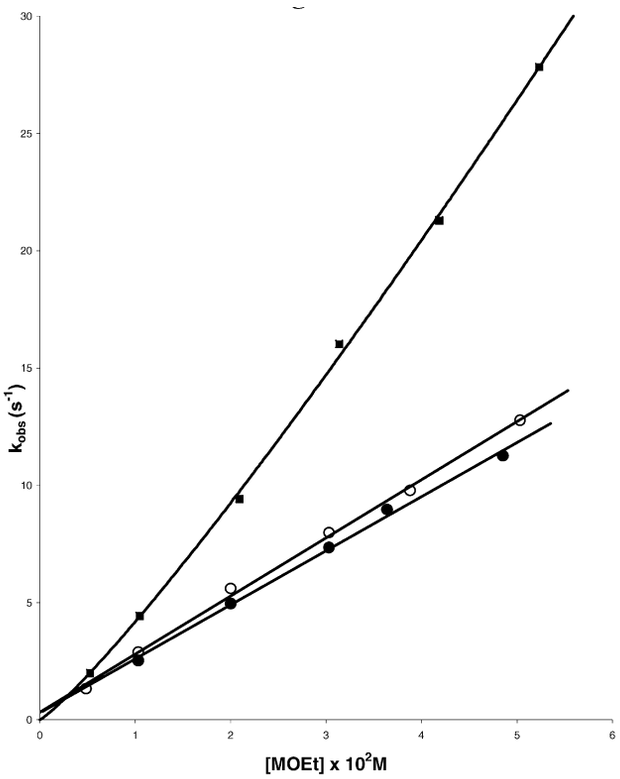

Fig. 1 Plots of the kinetic data for the reaction of **4a** with LiOEt (■) and KOEt (○) and with KOEt in the presence of excess 18-C-6 (●) in EtOH at 25 °C (see Tables 1 and 2).

and dissociated ions in the nucleophilic reaction, in which the ion-paired species is less reactive than dissociated ions. Contrariwise, the upward curvature of the k_{obs} *vs.* [LiOEt] plot herein reported, in which the order of reaction with respect to LiOEt > 1, is consistent with a model in which ion-paired LiOEt is more reactive than free EtO^-.

Dissection of rate constants

The kinetic data for the reaction of **4a** with LiOEt and KOEt in the absence of the complexing agent 18-C-6 are discussed in terms of Scheme 1 in which both free and ion-paired ethoxide contribute to the rate [eqn. (1)] and K_d (= $1/K_a$) is the ion-pair dissociation constant, defined in eqn. (2).

Table 3 Kinetic data for the reactions of **4b**–**f** with KOEt in anhydrous ethanol at 25.0 °C in the presence of excess 18-C-6[a]

Substrate	10^2 [KOEt]/M	10^2 [18-C-6]/M	k_{obs}/s^{-1}
4b	0.485	1.379	0.415
	1.031	2.217	0.919
	2.002	4.034	1.798
	3.034	6.201	2.746
	3.640	8.562	3.626
	4.854	10.75	5.193
4c	1.031	2.217	0.217
	2.002	4.034	0.459
	3.034	6.201	0.655
	3.640	8.562	0.879
	4.854	10.75	1.394
4d	0.8797	1.133	0.0586
	1.759	1.909	0.127
	2.606	3.010	0.202
	3.489	4.032	0.265
	4.399	5.106	0.357
4e	0.590	1.185	0.00483
	1.153	2.359	0.00998
	2.082	4.132	0.0196
	2.940	5.966	0.0279
	4.079	7.907	0.0396
	4.893	9.830	0.0500
4f	0.397	0.814	0.00134
	1.163	2.385	0.00430
	1.895	3.885	0.00747
	2.932	6.011	0.0119
	3.903	8.002	0.0165
	4.814	9.870	0.0216

[a] [18-Crown-6 ether]/[KOEt] ≥ 2.

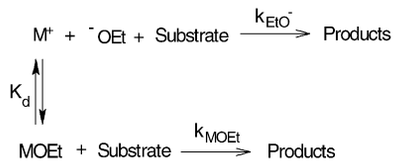

Scheme 1

$$k_{obs} = k_{EtO^-}[EtO^-]_{eq} + k_{MOEt}[MOEt]_{eq} \quad (1)$$

$$MOEt \overset{K_d}{\rightleftharpoons} M^+ + EtO^- \quad (2)$$

The rate constant for the reaction of free ethoxide with **4a** could conveniently be obtained by measuring the rate of reaction with KOEt in the presence of 18-C-6 where only free EtO^- will be present in solution, hence eqn. (1) simplifies to $k_{obs} = k_{EtO^-}[EtO^-]$. Now, a plot of k_{obs} *vs.* [KOEt] using the data in Table 2 gives slope, $k_{EtO^-} = 230 \pm 8\ M^{-1}\ s^{-1}$ ($R^2 = 0.997$).

To obtain the second-order rate constant for the reaction of the MOEt ion pair species, eqn. (1) is rewritten to give eqn. (3). According to eqn. (3), a plot of

$$k_{obs}/[EtO^-]_{eq} = k_{EtO^-} + k_{MOEt}[EtO^-]_{eq}/K_d \quad (3)$$

Table 4 Kinetic data for the reaction of **4e** with KOEt in anhydrous ethanol at 25.0 °C at varying [18-C-6][a]

10^3 [18-C-6]/M	[18-C-6]/[KOEt]	$10^3 k_{obs}/s^{-1}$	k_{obs}/[KOEt] ($M^{-1}\ s^{-1}$)[b]
0.000	0.000	5.821	1.007
3.134	0.542	5.247	0.9081
6.268	1.085	4.586	0.7937
12.24	2.170	4.562	0.8083
23.93	4.339	4.465	0.8094
35.90	6.508	4.362	0.7909
53.27	9.219	4.666	0.8076

[a] Initial [Substrate] = 6.14×10^{-4} M; initial [KOEt] = 5.78×10^{-3} M. [b] The value of this quantity (= k_{EtO^-}) of $0.80 \pm 0.01\ M^{-1}\ s^{-1}$obtained from this experiment may be compared with $k_{EtO^-} = 1.04 \pm 0.02\ M^{-1}\ s^{-1}$ derived by linear regression of the data in Table 3 for the reaction of **4e** with KOEt in the presence of a 2-fold excess of 18-C-6 (see text and Table 6).

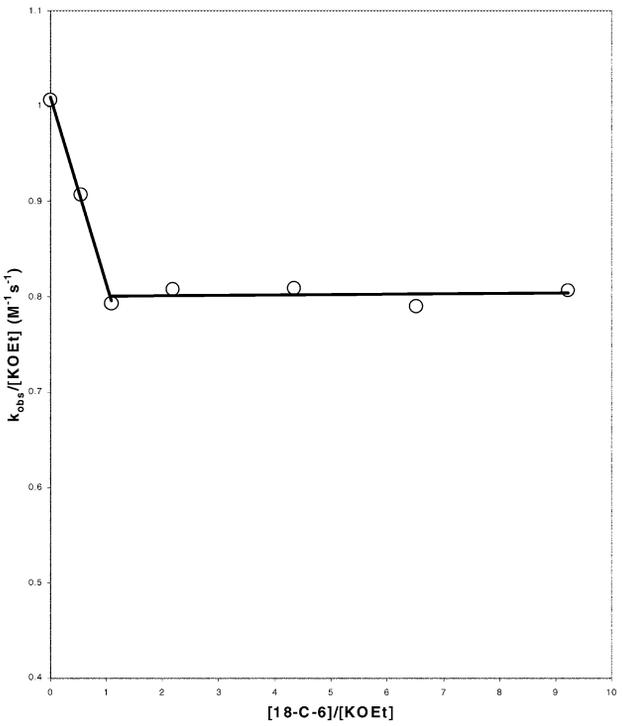

Fig. 2 Plots of the kinetic data for the reaction of **4e** with KOEt in the presence of increasing amounts of 18-C-6 in EtOH at 25 °C (see Table 4).

$k_{obs}/[EtO^-]_{eq}$ *vs.* $[EtO^-]_{eq}$ should be linear, with k_{MOEt}/K_d as slope. The values of K_d for LiOEt and KOEt are known from the literature (0.00472 M and 0.0111 M for LiOEt and KOEt, respectively, at 25 °C).[16] In order to apply eqn. (3), equilibrium concentrations of free ethoxide are calculated by eqn. (4) from the known initial stoichiometric

$$[EtO^-]_{eq} = 0.5\,[-K_d + (K_d^2 + 4K_d\,[MOEt]_0)^{1/2}] \quad (4)$$

concentrations of the metal ethoxide, since eqn. (5) applies. Values of $[EtO^-]_{eq}$

$$[MOEt]_0 = [EtO^-]_{eq} + [MOEt]_{eq} \quad (5)$$

obtained by this procedure for the different LiOEt and KOEt concentrations are included in Table 1.

For reaction of LiOEt, the resulting plot (Fig. 3) according to eqn. (3) is linear (R^2 = 0.996); its slope (= k_{LiOEt}/K_d) gives the ion-paired rate constant k_{LiOEt} = 648 ± 21 M^{-1} s^{-1}. The intercept yields k_{EtO^-} = 181 ± 41 M^{-1} s^{-1} but because of the large associated error, the k_{EtO^-} value (230 ± 8 M^{-1} s^{-1}) obtained above is adopted in the following.

Treatment of the data for reaction of KOEt according to eqns. (3)–(5), as for the procedure described for LiOEt, yields a plot (not shown) which tends to curve downwards at high [KOEt], giving a poor correlation coefficient. Hence k_{KOEt} = 255 ± 8 M^{-1} s^{-1} (R^2 = 0.996) was determined from eqn. (1) by linear regression analysis of the kinetic data for KOEt in Table 1, using the value of k_{EtO^-} = 230 M^{-1} s^{-1} obtained above in conjunction with $[EtO^-]_{eq}$ and $[KOEt]_{eq}$ values calculated from eqns. (4) and (5), respectively.

The resulting rate constants k_{EtO^-} and k_{MOEt} for the ethanolysis of **4a** by the three nucleophilic species EtO^-, KOEt and LiOEt are collected in Table 5 together with data for **1** and **2** from our previous studies. The k_{MOEt}/k_{EtO^-} ratios of 2.8 and 1.1 for Li^+ and K^+, respectively, for **4a** show moderate catalysis of the reaction by Li^+ and very weak catalysis by K^+, thereby giving quantitative expression to the relative catalytic strengths of Li^+ and K^+ demonstrated by the plots in Fig. 1.

Table 5 Calculated second-order rate constants for the ethanolysis of **4a**, **1** and **2** by free EtO^- (k_{EtO^-})[a] and the ion pairs KOEt (k_{KOEt}) and LiOEt (k_{LiOEt}) in anhydrous ethanol at 25 °C

Substrate	k_{EtO^-}/M^{-1} s^{-1}	k_{KOEt}/M^{-1} s^{-1}	k_{LiOEt}/M^{-1} s^{-1}
4a	230 ± 8	255 ± 8	648 ± 21
1[b]	0.980	4.84	24.0
2[c]	0.094	0.85	1.36

[a] Determined in the presence of 2-fold excess 18-C-6 (see text). [b] Taken from ref. 9*b*. [c] Taken from ref. 10*a*.

Table 6 Calculated rate constants for reaction of free EtO^- [a] with **4a**–**f** in anhydrous ethanol at 25 °C according to eqn. (1)

Substrate	k_{EtO^-}/M^{-1} s^{-1}
4a	230 ± 8
4b	99.1 ± 4.6
4c	24.4 ± 2.0
4d	8.36 ± 0.24
4e	1.04 ± 0.02
4f	0.46 ± 0.01

[a] Rates of the reactions of the substrates with KOEt were determined in the presence of 2-fold excess 18-C-6 and treated according to eqn. (1) (see text).

Table 7 Hammett ρ values (R^2) for leaving group variation in the reaction of EtO^- with aryl dimethylphosphinates (**4a**–**f**) in anhydrous ethanol at 25 °C

Substituent constant	ρ value (R^2)
σ	2.69 ± 0.13 (0.991)
σ°	2.77 ± 0.09 (0.996)
σ^-	1.77 ± 0.31 (0.890)

Values of k_{EtO^-} for the reactions of **4b**–**f** with free ethoxide (see Table 6) were obtained from plots of k_{obs} *vs.* [KOEt] using data collected in the presence of excess 18-C-6 (Table 3).

Linear free energy correlations and mechanism

To discuss the mechanism of the reaction and investigate leaving group effects on the rates of ethanolysis of substituted aryl dimethylphosphinates ($Me_2P(O)$–OPhX) in ethanol, Hammett plots were constructed using σ, σ° and σ^- constants in conjunction with the data in Table 6. As seen in Table 7, correlations with σ and σ° substituent constants are significantly better than with σ^- substituent constants (see Fig. 4 for the plot obtained with σ constants).

Correlation of rates with $\sigma(\sigma^\circ)$ substituent constants signifies that the incoming negative charge from the nucleophile is not delocalized onto the leaving group in the TS of the reaction. The moderately large $\rho(\rho^\circ)$ value of 2.7–2.8 indicates that the reaction is highly sensitive to electronic effects. It also suggests that a significant redistribution of charge occurs in the TS, resulting from partial delocalization of the π-electrons of the aryl oxygen onto the doubly bonded oxygen of the central phosphorus atom.[17] We propose that correlation with $\sigma(\sigma^\circ)$ substituent constants and the moderately high $\rho(\rho^\circ)$ value derived therefrom (Table 7) are consistent with a stepwise mechanism in which formation of the pentacoordinate intermediate **5** is rate-determining (Pathway A in Scheme 2). By contrast, the rates of the hydrolysis of $Me_2P(O)$–OPhX in 90% water–10% dioxane studied by Douglas and Williams[18] are correlated with σ^- substituent constants to yield a ρ^- value of 0.93, on which basis it was concluded that the reaction in water proceeds by a concerted mechanism (Pathway B, Scheme 2).[18]

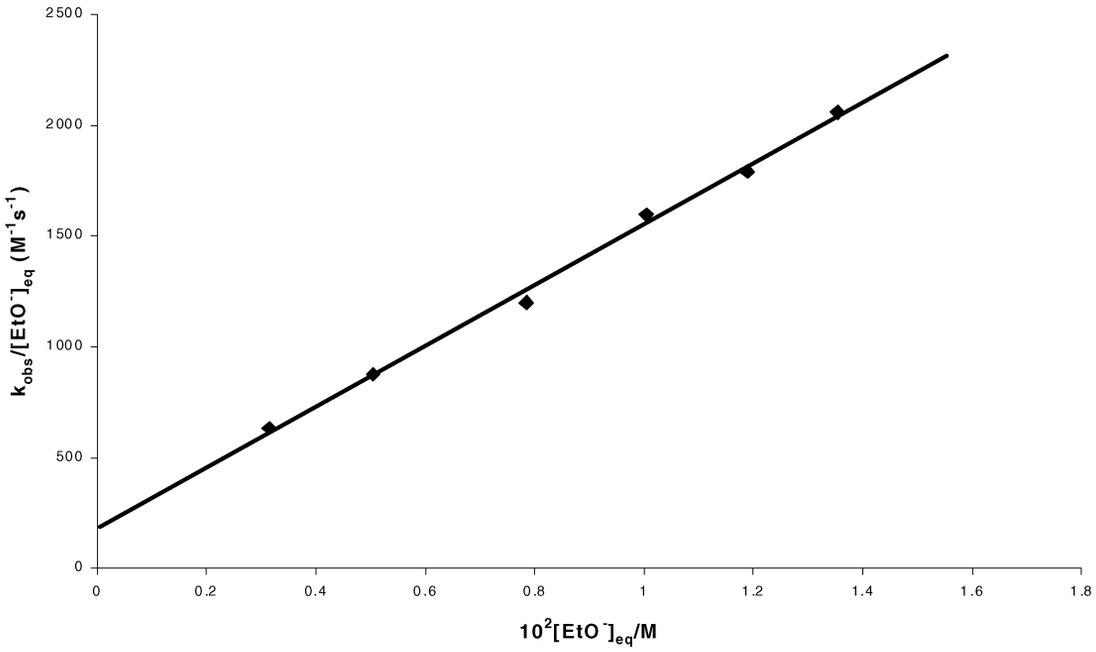

Fig. 3 Plot of $k_{obs}/[EtO^-]_{eq}$ *vs.* $[EtO^-]_{eq}$ for the reaction of **4a** with LiOEt in EtOH at 25 °C according to the ion pairing treatment of eqn. (3) (see text and Table 1).

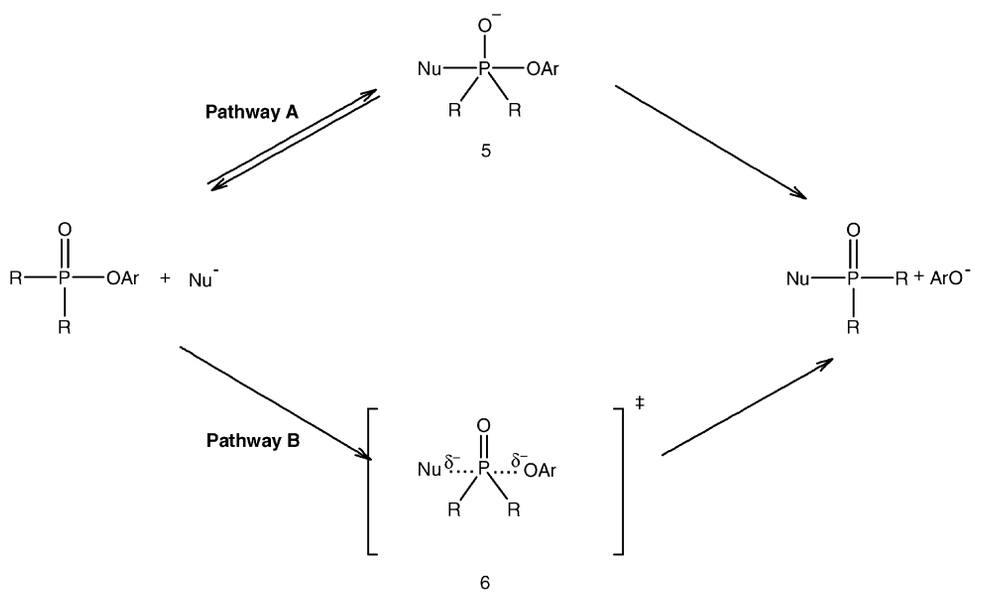

Scheme 2

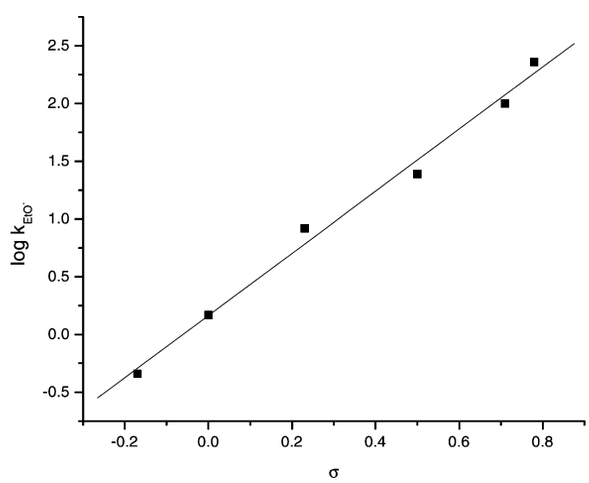

Fig. 4 Hammett σ–ρ plot for the reactions of **4a**–**f** with EtO^- in EtOH at 25 °C.

A valid comparison of the magnitude of $\rho(\rho^\circ)$ obtained in the present study with Williams' ρ^- value of 0.93 for the hydrolysis of $Me_2P(O)$–OPhX in aqueous dioxane would necessitate that the $\rho(\rho^\circ)$ value in ethanol be normalized with the $\rho_{eq}(\rho_{eq}^\circ)$ value for the reference equilibrium reaction in the same solvent. This is because electronic effects of substituents on rates and equilibria are more significant in ethanol than in water. Using the value of $\rho = 2.69$ (Table 7) and $\rho_{eq} = 1.96$ for the ionization of substituted benzoic acids in ethanol at 25 °C[19] gives normalized $\rho_n = \rho/\rho_{eq} = 1.37$. This normalized value is significantly higher than $\rho^- = 0.93$ measured by Williams for the corresponding hydrolysis reaction and accords with our view that the two reactions ($Me_2P(O)$–$OPhX/HO^-$ in aqueous dioxane and $Me_2P(O)$–$OPhX/EtO^-$ in ethanol) occur by different mechanisms.

A number of phosphinates have been shown in the literature to react by the stepwise mechanism, on the basis of linear Hammett $\sigma(\sigma^\circ)$ correlations and the moderately large $\rho(\rho^\circ)$ values derived therefrom. For example, the rates of alkaline hydrolysis of aryl diphenylphosphinothioates ($Ph_2P(O)$–SPhX)

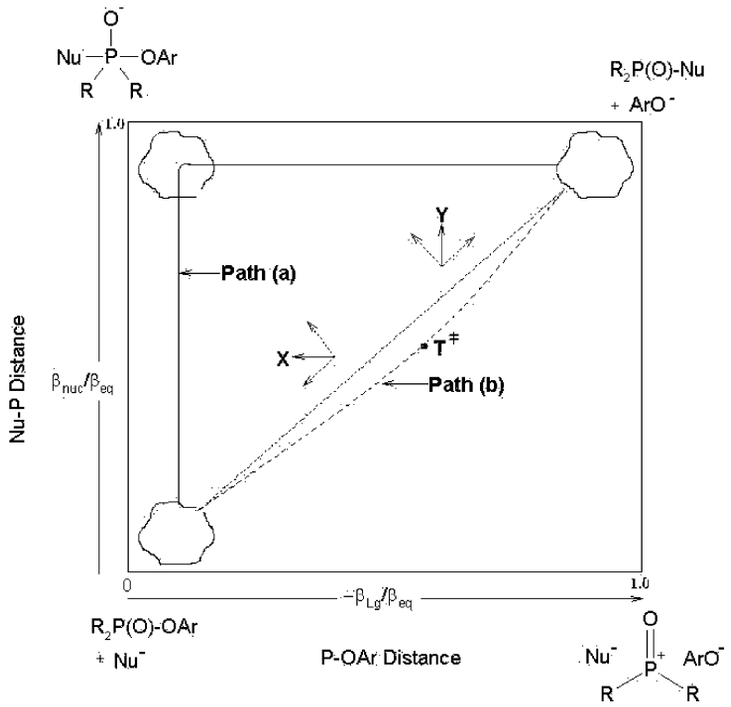

Fig. 5 Schematic three-dimensional potential energy diagram for the transfer of the R_2PO group between two nucleophiles to illustrate the effect of changing nucleophile and leaving group basicities in water and ethanol. Path (a) describes the route followed by reactions of $Me_2P(O)$–OPhX and $Ph_2P(O)$–OPhX substrates with nucleophiles in ethanol. Path (b) is followed by the concerted reaction of $Me_2P(O)$–OPhX with the HO^-/H_2O nucleophilic system, with the TS located at T‡. Changing the nucleophilic system to EtO^-/EtOH perturbs T‡ according to the dotted arrows, which show Hammond and anti-Hammond effects for increasing nucleophile and leaving group basicities. The resultant vectors ***x*** (for increasing nucleophile basicity) and ***y*** (for increasing leaving group basicity) show the net movements of T‡.

in 20% methanol–80% water were correlated with σ values rather than σ^- values, as in the present case, to yield a moderately high ρ value of 1.46.[20] The alkaline hydrolysis of the corresponding aryl diphenylphosphinates ($Ph_2P(O)$–OPhX) has been studied in other solvent systems; these substrates have also demonstrated better Hammett correlations with $\sigma(\sigma^\circ)$ than with σ^- constants, to give the following $\rho(\rho^\circ)$ values: 10% dioxane–90% water (ρ = 1.55),[21] 50% ethanol–50% water (ρ° = 1.93),[22] 60% acetone–40% water (ρ = 2.20),[17,20] and water (ρ° = 1.40).[22] It is important to note that the normalized ρ_n value (1.37) obtained in the present study for the ethanolysis of $Me_2P(O)$–OPhX is similar in magnitude to ρ values reported for the hydrolysis of $Ph_2P(O)$–OPhX and $Ph_2P(O)$–SPhX substrates in wholly aqueous or predominantly aqueous binary solvent mixtures. Williams[21] has pointed out that on the basis of such Hammett correlations it is difficult to make a clear distinction between a stepwise mechanism and a concerted process with a high degree of bond formation and little cleavage of the P–OPhX bond in the TS.

Hammett ρ values have generally been used to discuss S_N2-type TS structures. In general, S_N2 reactions at aliphatic carbon tend to give small ρ values which are either positive or negative.[23] Methyl transfer reactions show little or no effects of polar substituents on the central carbon atom; ρ values for methyl transfers with symmetrical transition states are ~ 0.[23–25] By analogy, concerted [S_N2(P)-type] reactions, which are accelerated by electron-withdrawing substituents, would be expected to give small positive ρ values. The prediction could be made that ρ values for a stepwise mechanism (Pathway A, Scheme 2) would be greater in magnitude than for the concerted [S_N2(P)-type] process (Pathway B, Scheme 2), as observed in the present study. Transmission of electronic effects of substituents on the leaving group phenyl moiety through the intact P–OAr bond in **7**/**7a** is more effective than through the partial bond of the concerted TS **6**/**6a**. It is noted that in aromatic nucleophilic substitution reactions, large ρ values in the range of 3.3–8.6 have been reported for the addition–elimination mechanism where the formation of an intermediate (addition) complex is rate limiting.[26]

Mechanism change with solvent for the $Me_2P(O)$–OPhX and $Ph_2P(O)$–OPhX systems

As shown above, ethanolysis of $Me_2P(O)$–OPhX occurs *via* a stepwise mechanism with rate-limiting formation of a pentacoordinate intermediate, contrasting with the concerted S_N2(P)-type mechanism reported for the corresponding hydrolysis reaction in 90% water–10% dioxane.[18] Although the nucleophiles HO^- (pK_a 15.74)[27a] and EtO^- (pK_a 16.0)[27a] have identical basicities in water, EtO^- is *ca.* 3 p*K* units more basic in ethanol than in water (pK_a in ethanol = 19.18).[27b] Change in solvent, from water to ethanol, and the consequent effect on basicity have therefore induced the change in mechanism reported in this study.

In the $Ph_2P(O)$–OPhX system, both ethanolysis[9] and hydrolysis reactions in 90% water–10% dioxane[21] and other binary aqueous solvents[20,22] occur by a stepwise mechanism. In contrast, however, reaction of the less basic PhO^- with $Ph_2P(O)$–OPhX esters in water occurs by a concerted mechanism,[28] but is stepwise in ethanol.[12c,29] This again is a solvent-induced change in mechanism, noting the enhanced basicity of PhO^- in ethanol (pK_a 15.76)[27b] relative to water (pK_a 9.96).[27a]

In the above examples, there are changes in the basicity of the base/solvent system, from HO^-/H_2O to EtO^-/EtOH in the $Me_2P(O)$–OPhX series and from PhO^-/H_2O to PhO^-/EtOH in the $Ph_2P(O)$–OPhX series. These basicity changes move the S_N2(P)-type TS toward structures with more bond formation and little or no bond rupture, in accord with the prediction of Williams[18,30] (see also ref. 31).

In the following sections, reactivities in the $Me_2P(O)$–OPhX and $Ph_2P(O)$–OPhX systems are compared. As well, the schematic reaction coordinate–energy diagram in Fig. 5 is used to demonstrate that structure–reactivity relationships of the β_{lg}/pK_{nuc} and β_{nuc}/pK_{lg} type, relating variations in nucleophile and

leaving group basicities to changes in TS structure, satisfactorily explain the observed change in mechanism in the present study.

(i) Reactivity in the $Me_2P(O)$–OPhX and $Ph_2P(O)$–OPhX systems. Second-order rate constants for nucleophilic attack by EtO^-, LiOEt, and KOEt are higher for **4a** than **1**, with k^{4a}/k^1 ratios of 235, 27, and 53 calculated from data in Table 6 for EtO^-, LiOEt, and KOEt, respectively. However, **1** would be expected to react faster than **4a** if the inductive effect of the substituents on P were the sole factor determining reactivity, in accord with Hammett σ_I substituent constants[32] for Ph and Me groups of 0.12 and −0.01, respectively. The opposite trend is observed, which points to the importance of steric factors in the nucleophilic reactions of **1**. In the hydrolysis reaction where the two substrate systems react by different mechanisms[18,21] (see above), the k^{4a}/k^1 ratio is much smaller (= 2.2). Imidazole catalysis of the hydrolysis reactions of these substrates occurs *via* general base catalysis for $Me_2P(O)$–OPhX[18] and nucleophilic catalysis for $Ph_2P(O)$–OPhX.[21] This difference in the mechanism of imidazole catalysis was attributed to steric crowding in the TS of the hydrolysis of $Ph_2P(O)$–OPhX esters.[18,21]

(ii) Effect of increase in nucleophile basicity on TS structure. The *y*-axis in Fig. 5 measures the Nu–P bond length and is identified with β_{nuc}, while the *x*-axis represents a measure of the P–OAr bond length and is identified with β_{lg}. The reactions in ethanol of $Me_2P(O)$–OPhX with EtO^- and of $Ph_2P(O)$–OPhX with EtO^- and PhO^-, all of which occur *via* rate-limiting formation of the pentacoordinate intermediate, follow the stepwise route described by Pathway (a) in Fig. 5.

The Brønsted characteristics for the hydrolysis of $Me_2P(O)$–OPhX in aqueous solution are now considered in order to locate the position of the concerted TS in Fig. 5. Douglas and Williams[18] give a value of $\beta_{nuc} = 0.41$ for this reaction, obtained with a series of oxygen nucleophiles; from these data,[18] a value of $\beta_{lg} = -0.47 \pm 0.03$ is calculated and thence $\beta_{eq} = 0.88$ according to eqn. (6). From these values of β_{nuc}, β_{lg}

$$\beta_{nuc} - \beta_{lg} = \beta_{eq} \quad (6)$$

$$\alpha = \beta_{nuc} \text{ (or } \beta_{lg})/\beta_{eq} \quad (7)$$

and β_{eq}, the Leffler indices α_{bf} = 0.41/0.88 = 0.47 and α_{br} = −0.47/0.88 = −0.53 are derived for bond formation and bond rupture, respectively, according to eqn. (7). These Brønsted characteristics demonstrate moderate bond formation and bond cleavage in a TS located at $T^{\neq}$ on Path (b) for the concerted hydrolysis of $Me_2P(O)$–OPhX, very close to the diagonal.

What then is the effect of change in the basicity of the nucleophile on the TS at $T^{\neq}$? Increasing the basicity of the nucleophile, *i.e.* changing from HO^- in H_2O (pK_a = 15.74[27a]) to EtO^- in EtOH (pK_a = 19.18[27b]), will lower the bottom corners in Fig. 5. This perturbation would tend to slide the TS at $T^{\neq}$ for the concerted reaction parallel to the reaction coordinate, toward the bottom left corner (the Hammond effect), as well as perpendicular to it, toward the associative left top corner (the anti-Hammond effect).[24,33] The resultant vector, indicated by arrow (***x***), says that β_{lg} becomes more positive, *i.e.* shifts toward the left on the β_{lg}/β_{eq} axis, equivalent to lesser separation of the leaving group in the TS. This movement of the TS in response to change in nucleophile basicity results from positive cross interaction between nucleophile and the leaving group, as elucidated by Jencks[24,33] *via* the cross-interaction coefficient p_{xy} in eqn. (8).

$$p_{xy} = -\partial\beta_{lg}/\partial pK_{nuc} = \partial\beta_{nuc}/\partial pK_{lg} \quad (8)$$

Examples of reduction in the extent of bond cleavage (*i.e.* shifts towards less negative β_{lg}) with increasing nucleophile basicity in phosphoryl transfer reactions have been furnished by Gorenstein[34] for the reaction of epimeric 2-(aryloxy)-2-oxydioxaphosphorinanes with a variety of nucleophilic species in 30% dioxane–70% water, and by Williams[28] for the reaction of $Ph_2P(O)$–OPhX with phenolate ions in aqueous dioxane solution.

Table 8 Comparison of the pK_a of substituted phenols in water and ethanol

Substituent	pK_a in water[a]	pK_a in ethanol[b]
4-Me	10.19	15.99
3-Me	10.08	15.83 (15.72)[c]
H	9.95	15.76 (15.58)[c]
4-Cl	9.38	14.90 (14.80)[c]
3-Cl	9.02	14.47 (14.40)[c]
4-Br	9.34	14.80 (14.69)[c]
4-EtOCO	8.50	13.78
3-MeCO	9.19	14.64
4-MeCO	8.05	13.26
4-CN	7.95	13.04
4-NO_2	7.14	12[c,d] (11.7 ± 2)[c,e]

[a] Values determined at 25 °C, taken from ref. 31*b*. [b] Values determined at 25 °C, taken from ref. 31*a*. [c] Values at 22 °C given by G. Guanti, G. Cevasco, S. Thea, C. Dell'Erba and G. Petrillo, *J. Chem. Soc., Perkin Trans. 2*, 1981, 327. [d] Estimated value. [e] Calculated from a correlation of pK_a values in water and ethanol.

(iii) Effect of enhanced basicity of the leaving group on TS structure. Phenols are generally more acidic in water than ethanol by *ca.* 5 p*K* units (see Table 8 for a comparison of the pK_a values of several phenols in water and ethanol). The change from the $Me_2P(O)$–OPhX/HO^- system in water to $Me_2P(O)$–OPhX/EtO^- system in ethanol involves a significant change in the basicity of the leaving group phenoxide as well, in addition to the change in nucleophile basicity considered above. Such an increase in basicity is equivalent to making the nucleofuge a poorer one.

The change from a less basic leaving group (phenoxide in water) to a more basic leaving group (phenoxide in ethanol), in the present work, raises the energy of the right side of Fig. 5 relative to the left. For the concerted reaction on Path (b), the parallel Hammond effect moves the TS at $T^{\neq}$ to the upper right, while the anti-Hammond effect slides $T^{\neq}$ to the upper left. The resultant vector, arrow (***y***), signifies an increase in β_{nuc} with increased basicity of the leaving group, equivalent to greater bond formation between the nucleophile and the P center in the TS. This is a consequence of cross interactions between the nucleophile and the leaving group according to eqn. (8).[24,33] Examples of this phenomenon have been reported by Jencks[35] for phosphoryl transfer in water between amine nucleophiles and oxygen and nitrogen leaving groups, and by Gorenstein[34] for the hydrolysis of epimeric 2-(aryloxy)-2-oxydioxaphosphorinanes in 30% dioxane–70% water.

(iv) Net effect of changes in nucleophile and nucleofuge basicity on the concerted TS. The combined effect of vectors (***x***) and (***y***) on $T^{\neq}$ for the nucleophilic reaction of $Me_2P(O)$–OPhX is to move the TS, from concerted towards the pentacoordinate intermediate structure at the top-left corner in Fig. 5, *i.e.* to Path (a) for reactions involving poor leaving groups and strongly basic nucleophiles.

The above changes in TS structure with changes in nucleophile and leaving group basicity, illustrated in Fig. 5, satisfactorily explain the change in mechanism encountered in the nucleophilic reactions of $Me_2P(O)$–OPhX. As well, they show that a spectrum of transition states exists, resulting from positive interactions between the nucleophile and the leaving group in the TS. As the nucleophile becomes more basic, bond fission to the nucleofuge becomes progressively less advanced in the

Table 9 Rate constants for reaction by free EtO^- and ion pairs and free energies of alkali metal ion stabilization of EtO^- (δG_{ip}), transition states (δG_{ts}), and the net catalytic effect (ΔG_{cat}) for the reaction of EtO^- with **1**, **2** and **4a** in ethanol at 25 °C. Free energies are given in kJ mol^{-1}

	$k/M^{-1}\ s^{-1}$			δG_{ip}	δG_{ts}			ΔG_{cat}		
Species	**1**	**2**	**4a**	EtO^-	**1**	**2**	**4a**	**1**	**2**	**4a**
EtO^-	0.980	0.094	230							
Li^+	24.0	1.36	648	−13.3	−21.2	−19.7	−15.8	−7.9	−6.4	−2.5
K^+	4.84	0.85	248	−11.2	−15.1	−16.4	−11.4	−3.9	−5.2	−0.2

TS. Conversely, as the nucleofuge becomes poorer, bond formation becomes progressively more advanced in the TS. Both of these effects act in the same direction for the $Me_2P(O)$–OPhX/EtO^- system, and these result in the change of mechanism recorded in this study.

Ground state *versus* transition state stabilization by alkali metal ions and the mechanism of catalysis

Metal ion catalysis in these systems implies that participation by alkali metal ions decreases the free energy of activation of the reaction, which can result from the interaction of the metal ions with the ground state, the TS, or both. The present discussion follows our earlier treatment of alkali metal ion catalysis,[9–11] which assumes that the interaction between the metal ions and the substrates is negligible, *i.e.* M^+/EtO^- interaction, measured by K_a (= K_d^{-1}), is regarded as the dominant ground state interaction.

Interactions between metal ions and the TS have been discussed[9–11] in terms of Kurz's model[36a] for the characterization of the transition states of catalyzed reactions; different forms of this treatment have been applied by Mandolini[36b] and Tee.[36c] A virtual association constant of a catalyst with the transition state, K_a', is calculated by means of the thermodynamic cycle in Scheme 3 and according to eqn. (9). The free energies of

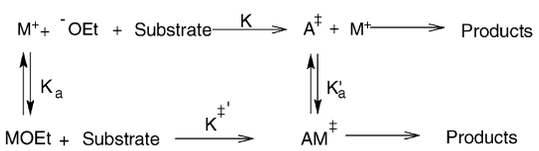

Scheme 3

$$K_a' = k_{EtOM}\, K_a/k_{EtO^-} \qquad (9)$$

$$\Delta G_{cat} = \Delta G_c^{\ddagger} - \Delta G_u^{\ddagger} = \delta G_{ts} - \delta G_{ip} \qquad (10)$$

stabilization, δG_{ts} and δG_{ip}, are obtained from K_a' and K_a, respectively, to give ΔG_{cat}, the net catalytic effect of the metal ion, according to eqn. (10). Values of ΔG_{cat}, δG_{ts} and δG_{ip} obtained for the reaction of **4a** are presented in Table 9; this table also includes corresponding data for **1** and **2** for comparison. The overall relationship between ground state and transition state stabilization is illustrated in Fig. 6.

ΔG_{cat} values for **4a** are −2.5 and −0.2 kJ mol^{-1} for Li^+ and K^+, respectively. These values indicate moderate catalysis by

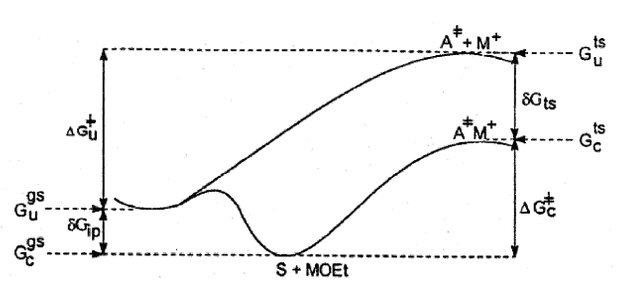

Fig. 6 Free energies involved in the uncatalyzed and metal ion catalyzed reactions of substrate S with alkali metal ethoxides.

Li^+ and a very weak effect for K^+, giving the selectivity order of $Li^+ > K^+$. The catalytic effect of Li^+ is smaller for **4a** than that observed in our earlier studies for **1** and **2**,[9a,10a] ΔG_{cat} values (in kJ mol^{-1}) being −7.9 (Li^+) and −3.9 (K^+) for **1**, and −6.4 (Li^+) and −5.2 (K^+) for **2**. In particular, comparing the phosphinate esters **1** and **4a**, it is seen that the most reactive substrate (**4a**) towards ethanolysis (k_{EtO^-} = 230 and 0.98 $M^{-1}\ s^{-1}$ for **4a** and **1**, respectively) is the least susceptible to metal ion catalysis. The lower sensitivity of **4a** to alkali metal ion catalysis, relative to **1**, is highlighted by the following k_{MOEt}/k_{EtO^-} ratios: 2.8 (Li^+) and 1.1 (K^+) for **4a**, and 24.5 (Li^+) and 4.9 (K^+) for **1**.

We had earlier[10a,11b,12b,12d,13] related observed selectivities in the ethanolysis of different P-, S-, C-centered esters to the selectivity patterns of alkali metal cations for ion-exchange resins and glass electrodes as elucidated by Eisenman[37] in his theory of ion-exchange selectivity. Our analysis showed that electrostatic interactions are dominant over solvent rearrangement in the nucleophilic reactions of phosphorus esters manifesting alkali metal ion catalysis, resulting in the selectivity order $Li^+ > Na^+ > K^+ > Cs^+$, while the reverse order, *i.e.* $Cs^+ > K^+ > Na^+ > Li^+$, obtains for sulfonate esters.[10a,11b,12b,12d,13] Significantly, a linear relationship was shown[10a,12b,12d] to exist between δG_{ts} and the inverse of the crystal radius of M^+ for the ethanolysis of **1** and **2**. The metal ion selectivity obtained in this work is generally in accord with the prediction based on Eisenman's theory, although it is noted that ΔG_{cat} values obtained for **4a** are small in comparison to **1** and **2** (see Table 9). In accord with the electrostatic mode of stabilization discussed above, the smaller Li^+ cation, with a higher charge/mass ratio, binds more strongly than the larger K^+.

Greater stabilization of the TS relative to the initial state gives the clue that the mechanism of catalysis involves chelation of the metal ion, which is stronger with the TS than with the initial state. Fig. 7 displays the initial state, the TS, and the pentacoordinate intermediate for the uncatalyzed and catalyzed reactions. The TS for the uncatalyzed (**8**) and catalyzed (**10**) reactions, as shown, are idealized structures in which the incoming negative charge is equally shared between the nucleophile and substrate oxygens. In principle, the TS for the uncatalyzed reaction could have structures resembling the initial state or the pentacoordinate intermediate (**9**), depending on whether it is early or late. Similarly, the TS for the catalyzed reaction could resemble the initial state (early TS) or the metal-coordinated intermediate **11** (late TS). An early TS for the catalyzed reaction (depicted as **12**) will derive very little stabilization from M^+ because of the minimal amount of negative charge available on the P–O oxygen for chelation. Metal ion catalysis for such a reaction will therefore be small in magnitude. Conversely, a late TS for the catalyzed reaction (depicted as **13**) will derive substantial stabilization through chelation with M^+ because of the significant amount of negative charge resident on the P–O oxygen.

It is therefore reasonable to conclude that the observed reduced susceptibility of **4a** to metal ion catalysis, relative to **1**, is indicative that metal catalyzed ethanolysis of **4a** proceeds with an earlier TS than the corresponding reaction of **1**. As discussed above, **4a** is significantly more reactive than **1** towards free ethoxide ion, k^{4a}/k^{1} = 235, consistent with an earlier TS for the ethanolysis of **4a** than for **1**, according to the Hammond postulate.

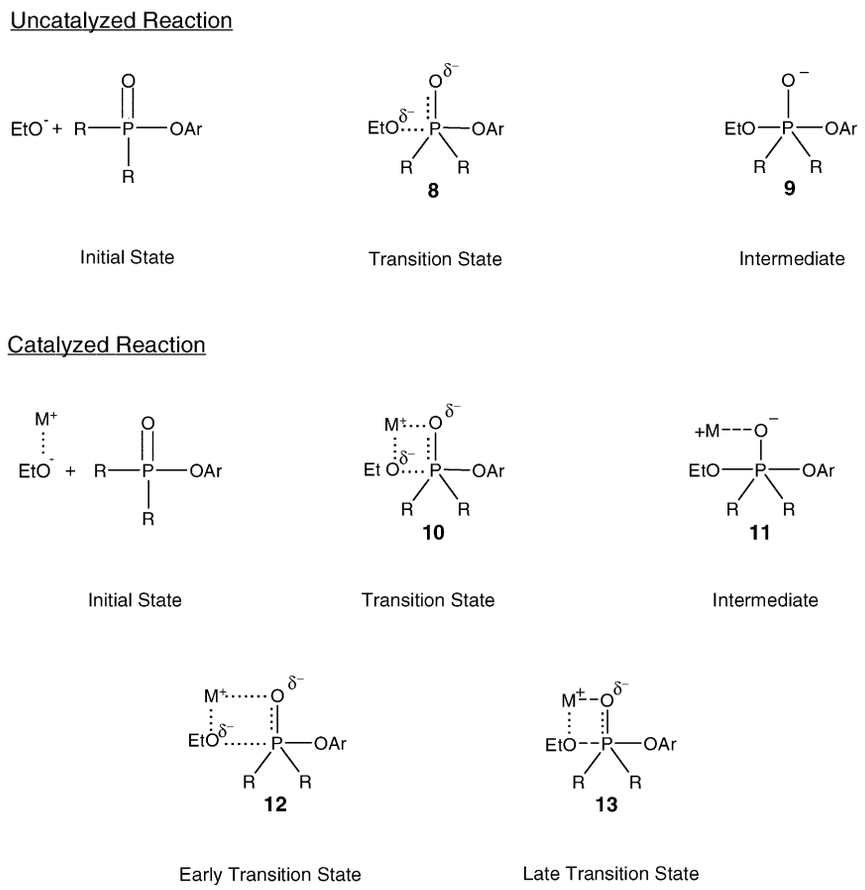

Fig. 7 Initial states, transition states, and intermediates for the uncatalyzed and metal ion-catalyzed ethanolysis of $R_2P(O)$–OAr (R = Me or Ph).

Conclusions

Our study concludes that ethanolysis of $Me_2P(O)$–OPhX occurs by a stepwise mechanism involving rate-determining formation of a pentacoordinate intermediate. The apparent contrast whereby the hydrolysis of $Me_2P(O)$–OPhX in water occurs *via* a concerted mechanism while the corresponding ethanolysis reaction is a stepwise process is examined by structure–reactivity correlations of the Jencks–More O'Ferrall type. The analysis reveals cross-interactions between the nucleophile and the leaving group in the concerted TS of the hydrolysis reaction. As a consequence of these interactions, enhanced basicities of the nucleophile and the leaving group in ethanol decrease the extent of bond rupture and increase the degree of bond formation in the TS. A duality of mechanism in the nucleophilic substitution reactions at the P center of $Me_2P(O)$–OPhX exists over a wide range of nucleophile and leaving group basicities within a spectrum of transition states.

The kinetic data presented herein reveal moderate and weak catalysis by Li^+ and K^+, respectively. The mode of stabilization is electrostatic in nature, the chelate effect of the metal ions on the TS being inversely proportional to their crystal radii. Although the selectivity order $Li^+ > K^+$ observed is similar to previous reports from our laboratory for the ethanolysis of phosphorus-based substrates, susceptibility to metal ion catalysis is lower for **4a** than **1** and **2**. The differential sensitivity of the structurally similar **1** and **4a** to alkali metal catalysis provides a clue to dissimilar transition states for the catalyzed reaction of both substrates.

Experimental

Materials

Anhydrous ethanol was obtained by refluxing absolute ethanol with magnesium turnings in the presence of iodine followed by distillation. Solutions of potassium ethoxide were prepared by dissolving clean potassium metal in dry ethanol at 0 °C under nitrogen. Lithium ethoxide solutions were made in a similar manner by dissolving lithium hydride (Alfa-Ventron) in anhydrous ethanol; the insoluble lithium carbonate formed was removed by filtration. The concentration of the base solutions was determined by titration with anhydrous potassium hydrogen phthalate (Mathieson, Coleman/Bell). 18-C-6, purchased from Parish Chemicals, was recrystallized from acetonitrile and dried over P_2O_5 *in vacuo* prior to use.

Synthesis of substrates

The substituted phenyl dimethylphosphinate esters investigated in this study were prepared from the parent phenols and dimethylphosphinoyl chloride using a general procedure described by Williams.[18] Dimethylphosphinoyl chloride was first obtained through a series of known reactions according to eqn. (11). Bisdimethylphosphinyl

$$CH_3MgBr + P(S)Cl \rightarrow \underset{\mathbf{14}}{\left[(CH_3)_2P(S)\right]_2} \rightarrow \underset{\mathbf{15}}{Me_2P(O)OH} \rightarrow \underset{\mathbf{16}}{Me_2P(O)Cl} \quad (11)$$

disulfide (**14**) was prepared according to the method of Parshall[38] and was recrystallized from ethanol as white needles, mp 229 °C (lit.,[38] 229 °C). Dimethylphosphinic acid (**15**) was obtained by the method of Reinhardt *et al.*[39] as white needles, mp 87.5–89 °C (lit.,[39] 88.5–90.5 °C). The chloride **16** was obtained by heating an equimolar mixture of **15** and PCl_5 at 115 °C for 1 h under nitrogen; the reaction mixture was further stirred for 10 h at room temperature and then distilled to yield a yellow oil which solidified on standing, mp 66 °C (lit.,[40] 66 °C).

Phenyl dimethylphosphinate esters were then prepared by the following general method described for 4-nitrophenyl

dimethylphosphinate. Equimolar quantities of 4-nitrophenol, pyridine, and dimethylphosphinoyl chloride were stirred in dichloromethane for 12 h in an atmosphere of nitrogen. The white precipitate of pyridinium chloride was filtered off in an inert atmosphere in a glove box. The filtrate was dried with $MgSO_4$ and the solvent evaporated off to give a red oil which solidified on trituration with dry ether. Three recrystallizations from dichloromethane gave the pure product **4a**. Liquid products were purified by distillation under vacuum. The products gave ^1H and ^{13}C NMR spectra consistent with the structures of the esters. The boiling/melting points obtained for the esters are as follows: 4-nitrophenyl dimethylphosphinate (**4a**), mp 98–100 °C, with decomposition (lit.,[18] 97–101 °C); 3-nitrophenyl dimethylphosphinate (**4b**), mp 80–82 °C, with decomposition (lit.,[18] 81–84 °C); 4-acetylphenyl dimethylphosphinate (**4c**), bp 174–176 °C, 1.25 mm Hg (lit.,[18] 219–228 °C, 30 mm Hg); 4-chlorophenyl dimethylphosphinate (**4d**), bp 110 °C, 0.77 mm Hg (lit.,[18] 182–184 °C, 27 mm Hg); phenyl dimethylphosphinate (**4e**), bp 102–106 °C, 0.70 mm Hg (lit.,[18] 164–166 °C, 27 mm Hg); and 4-methylphenyl dimethylphosphinate (**4f**), bp 141–142 °C, 2.17 mm Hg (lit.,[18] 160–170 °C, 15 mm Hg).

Kinetic method

The rates of reaction in anhydrous ethanol were followed spectrophotometrically by monitoring the formation of the appropriate phenoxide ion at 25 °C under pseudo-first order conditions, with base concentrations at least 20-fold in excess of the substrate. Kinetics were performed, in part, using a Beckman DU-8 or Perkin-Elmer Lambda-5 spectrophotometer, equipped with thermostatted cell holders which maintained the temperature inside the 10 mm quartz cuvette at 25 ± 0.1 °C. Relatively fast kinetic experiments were monitored using a Hi-Tech stopped-flow module equipped with a thermostatted water bath coupled to a McPherson monochromator and Can-Tech transient recorder. Spectral traces were displayed on a Hewlett-Packard oscilloscope and the data were treated directly by a Commodore CBM 8032 computer. Typically, run solutions of substrates were made up just prior to kinetic runs which were generally performed in replicate and followed for 10 half-lives. First-order rate constants, k_{obs}, were reckoned from linear plots of ln $(A_\infty - A_t)$ *vs.* time.

Acknowledgements

Support of this research by the Natural Sciences and Engineering Research Council of Canada (NSERC) is gratefully acknowledged. KGA is the recipient of the Queen's University Graduate Student Fellowship.

References

1 W. N. Lipscombe and N. Slater, *Chem. Rev.*, 1996, **96**, 2375.
2 A. Fersht, *Enzyme Structure and Mechanism*, W. H. Freeman and Co., New York, 2nd Edition, 1985.
3 G. R. J. Thatcher and R. Kluger, *Adv. Phys. Org. Chem.*, 1989, **25**, 99.
4 R. Krämer, *Coord. Chem. Rev.*, 1999, **182**, 243.
5 (*a*) C. Vichard and T. A. Kaden, *Inorg. Chim. Acta*, 2002, **337**, 173; (*b*) P. Hendry and A. M. Sargeson, *Inorg. Chem.*, 1990, **29**, 92 and references cited therein; (*c*) K. A. Deal and J. N. Burstyn, *Inorg. Chem.*, 1996, **35**, 2792.
6 (*a*) D. Herschlag and W. P. Jencks, *J. Am. Chem. Soc.*, 1987, **109**, 4665; (*b*) I. E. Catrina and A. C. Hengge, *J. Am. Chem. Soc.*, 1999, **121**, 2156.
7 (*a*) J. S. Tsang, A. A. Neverov and R. S. Brown, *J. Am. Chem. Soc.*, 2003, **125**, 1559; (*b*) J. S. Tsang, A. A. Neverov and R. S. Brown, *J. Am. Chem. Soc.*, 2003, **125**, 7602.
8 J. J. R. Fraùsto da Silva and R. J. P. Williams, *The Biological Chemistry of the Elements*, Clarendon Press, Oxford, 1993, pp. 230–242.
9 (*a*) E. Buncel, E. J. Dunn, R. A. B. Bannard and J. G. Purdon, *J. Chem. Soc., Chem. Commun.*, 1984, 162; (*b*) E. J. Dunn and E. Buncel, *Can. J. Chem.*, 1989, **67**, 1440; (*c*) E. J. Dunn, R. Y. Moir and E. Buncel, *Actual. Fis.-Quim. Org.*, 1991, 110.
10 (*a*) R. Nagelkerke, G. R. J. Thatcher and E. Buncel, *Org. Biomol. Chem.*, 2003, **1**, 163; (*b*) E. Buncel, R. Nagelkerke and G. R. J. Thatcher, *Can. J. Chem.*, 2003, **81**, 53; (*c*) R. Nagelkerke, M. J. Pregel, E. J. Dunn, G. R. J. Thatcher and E. Buncel, *Org. React. (Tartu)*, 1995, **105**, 11.
11 (*a*) M. J. Pregel and E. Buncel, *J. Am. Chem. Soc.*, 1993, **115**, 10; (*b*) M. J. Pregel and E. Buncel, *J. Org. Chem.*, 1991, **56**, 5583; (*c*) M. J. Pregel and E. Buncel, *J. Chem. Soc., Perkin Trans. 2*, 1991, 307.
12 (*a*) M. J. Pregel, E. J. Dunn and E. Buncel, *J. Am. Chem. Soc.*, 1991, **113**, 3545; (*b*) M. J. Pregel, E. J. Dunn and E. Buncel, *Can. J. Chem.*, 1990, **68**, 1846; (*c*) E. J. Dunn, R. Y. Moir, E. Buncel, J. G. Purdon and R. A. B. Bannard, *Can. J. Chem.*, 1990, **68**, 1837; (*d*) E. Buncel and M. J. Pregel, *J. Chem. Soc., Chem. Commun.*, 1989, 1566.
13 M. J. Pregel, E. J. Dunn, R. Nagelkerke, G. R. J. Thatcher and E. Buncel, *Chem. Soc. Rev.*, 1995, **24**, 445.
14 (*a*) J. R. Jones, *Prog. React. Kinet.*, 1973, **7**, 1; (*b*) A. Papoutsis, G. Papanastasiou, J. Jannakoudakis and C. Georgulis, *J. Chim. Phys.*, 1985, **82**, 913; (*c*) K. J. Msayib and C. I. F. Watt, *Chem. Soc. Rev.*, 1992, **21**, 237.
15 (*a*) C. C. Evans and S. Sugden, *J. Chem. Soc.*, 1949, 270; (*b*) J. R. Bevan and C. B. Monk, *J. Chem. Soc.*, 1956, 1396; (*c*) P. Jones, P. Harrison and L. Wynne-Jones, *J. Chem. Soc., Perkin Trans. 2*, 1979, 1679; (*d*) P. Beronius and L. Pataki, *Acta Chem. Scand., Ser. A*, 1979, **33**, 675; (*e*) N. N. Lichtin and K. N. Rao, *J. Am. Chem. Soc.*, 1961, **83**, 2417.
16 J. Barthel, J.-C. Justice and R. Wachter, *Z. Phys. Chem. Neu. Folge*, 1973, **84**, 113.
17 P. Haake, D. R. McCoy, W. Okamura, S. R. Alpha, S.-Y. Wong, D. A. Tyssee, J. P. McNeal and R. D. Cook, *Tetrahedron Lett.*, 1968, 5243.
18 K. T. Douglas and A. Williams, *J. Chem. Soc., Perkin Trans. 2*, 1976, 515.
19 H. H. Jaffe, *Chem. Rev.*, 1953, **53**, 191.
20 R. D. Cook and L. Rahhal-Arabi, *Tetrahedron Lett.*, 1985, 3147.
21 A. Williams and R. A. Naylor, *J. Chem. Soc. (B)*, 1971, 1967.
22 B. I. Istomin, N. A. Sakhdrukova, A. V. Kalabina and Y. I. Sukhorkov, *Zh. Obsch. Khim.*, 1982, **52**, 2011; *Engl. Transl.* p. 1787.
23 S. R. Hartshorn, *Aliphatic Nucleophilic Substitution*, Cambridge University Press, Cambridge, 1973, pp. 88–90.
24 W. P. Jencks, *Chem. Rev.*, 1985, **85**, 511.
25 W. J. Albery and M. M. Kreevoy, *Adv. Phys. Org. Chem.*, 1978, **16**, 87.
26 J. Miller, *Aromatic Nucleophilic Substitution*, Elsevier, Amsterdam, 1968, Chapter 4.
27 (*a*) W. P. Jencks and J. Regenstein, in *Handbook of Biochemistry*, Ed. H. A. Sober, The Chemical Rubber Co., Cleveland, 1970, 2nd Edition, Section J-187; (*b*) I.-H. Um, Y.-J. Hong and D.-S. Kwon, *Tetrahedron*, 1997, **53**, 5073.
28 N. Bourne, E. Chrystiuk, A. M. Davis and A. Williams, *J. Am. Chem. Soc.*, 1988, **110**, 1890.
29 E. Buncel and E. J. Dunn, unpublished results.
30 (*a*) A. Williams, *Acc. Chem. Res.*, 1989, **22**, 387 and references cited therein; (*b*) N. Bournes, E. Chrystiuk, A. M. Davies and A. Williams, *J. Am. Chem. Soc.*, 1988, **110**, 1890; (*c*) S. A. Ba-Saif, M. A. Waring and A. Williams, *J. Chem. Soc., Perkin Trans. 2*, 1991, 1653.
31 J. E. Omakor, I. Onyido, G. W. vanLoon and E. Buncel, *J. Chem. Soc., Perkin Trans. 2*, 2001, 324.
32 M. Charton, *Prog. Phys. Org. Chem.*, 1987, **16**, 287.
33 D. A. Jencks and W. P. Jencks, *J. Am. Chem. Soc.*, 1977, **99**, 7948.
34 R. Rowell and D. Gorenstein, *J. Am. Chem. Soc.*, 1981, **103**, 5894.
35 (*a*) D. Herschlag and W. P. Jencks, *J. Am. Chem. Soc.*, 1989, **111**, 7587 and references cited therein; (*b*) W. P. Jencks, M. T. Haber, D. Herschlag and K. L. Nazaretian, *J. Am. Chem. Soc.*, 1986, **108**, 479; (*c*) M. T. Skoog and W. P. Jencks, *J. Am. Chem. Soc.*, 1984, **106**, 7597.
36 (*a*) J. L. Kurz, *J. Am. Chem. Soc.*, 1963, **85**, 987; (*b*) R. Cacciapaglia and L. Mandolini, *Chem. Soc. Rev.*, 1993, **22**, 221; (*c*) O. S. Tee, *Adv. Phys. Org. Chem.*, 1994, **29**, 1.
37 D. Eisenman, *Biophys. J. Suppl.*, 1962, **2**, 259.
38 G. W. Parshall, *Org. Synth.*, 1965, **45**, 102.
39 H. Reinhardt, D. Bianchi and D. Molle, *Chem. Ber.*, 1957, **90**, 1656.
40 K. A. Pollart and H. J. Harwood, *J. Org. Chem.*, 1962, **27**, 4446.